

An interpolatory ansatz captures the physics of one-dimensional confined Fermi systems

M. E. S. Andersen¹, A. S. Dehkharghani¹, A. G. Volosniev^{2,1}, E. J. Lindgren^{3,4}, and N. T. Zinner^{1,*}

¹Department of Physics and Astronomy, Aarhus University, DK-8000 Aarhus C, Denmark

²Institut für Kernphysik, Technische Universität Darmstadt, 64289 Darmstadt, Germany

³Theoretische Natuurkunde, Vrije Universiteit Brussel, and International Solvay Institutes, Pleinlaan 2, B-1050 Brussels, Belgium

⁴Physique Théorique et Mathématique, Université Libre de Bruxelles, Campus Plaine C.P. 231, B-1050 Bruxelles, Belgium

*zinner@phys.au.dk

ABSTRACT

Interacting one-dimensional quantum systems play a pivotal role in physics. Exact solutions can be obtained for the homogeneous case using the Bethe ansatz and bosonisation techniques. However, these approaches are not applicable when external confinement is present. Recent theoretical advances beyond the Bethe ansatz and bosonisation allow us to predict the behaviour of one-dimensional confined systems with strong short-range interactions, and new experiments with cold atomic Fermi gases have already confirmed these theories. Here we demonstrate that a simple linear combination of the strongly interacting solution with the well-known solution in the limit of vanishing interactions provides a simple and accurate description of the system for all values of the interaction strength. This indicates that one can indeed capture the physics of confined one-dimensional systems by knowledge of the limits using wave functions that are much easier to handle than the output of typical numerical approaches. We demonstrate our scheme for experimentally relevant systems with up to six particles. Moreover, we show that our method works also in the case of mixed systems of particles with different masses. This is an important feature because these systems are known to be non-integrable and thus not solvable by the Bethe ansatz technique.

Introduction

Understanding the properties of low-dimensional systems is not merely an academic pursuit. Technologically promising systems such as nanotubes, nanowires, and organic conductors have one-dimensional nature¹⁻³, while there is much evidence that high-temperature superconductors owe their spectacular properties to an effective two-dimensional structure^{4,5}. However, in the case of interacting particles in one dimension there are still many outstanding fundamental issues in their quantum mechanical description. An avenue within which these problems can be studied is that of cold atomic gases^{6,7} where experiments in one-dimensional (1D) confinement can be performed with tunable interactions for systems of bosons⁸⁻¹⁴ or fermions¹⁵. Most recently, 1D Fermi systems have been constructed with full control over the particle number¹⁶ and thus engineered few-body systems are now available. This provides opportunities to study pairing, impurity physics, magnetism, and strongly interacting particles from the bottom up¹⁷⁻²¹.

The role of strong interactions in important quantum phenomena such as superconductivity and magnetism drives research into the regime of strong interactions also for 1D systems. In this respect, new theoretical approaches to confined quantum systems with strong short-range interactions have been proposed in the last couple of years²²⁻²⁹. Within these new developments it has become clear that the strongly interacting limit has an emergent Heisenberg spin model description. While this was realized some time ago for the case of a homogeneous system³⁰, in the presence of confinement the Heisenberg model obtained has non-trivial nearest-neighbour interactions that depend on the confining potential. This can be exploited for tailoring systems to have desired static and dynamic properties²⁵. In the opposite limit where we have vanishing interactions, confined 1D systems are trivially solved as the single-particle Schrödinger equation can be solved numerically to any desired level of accuracy. The natural question to ask is how to describe 1D systems with interaction strengths that are somewhere in the region between the two extreme limits?

In this paper, we propose a deceptively simple ansatz that linearly combines our knowledge of the weakly and strongly interacting limits. As an ansatz containing just two wave functions it is much easier to work with as compared to entirely numerical approaches, which typically have the solution represented on a large basis set with many non-zero contributions.

To describe the main idea we will focus on two-component Fermi systems of N_\uparrow particles with spin projection up and N_\downarrow particles with spin projection down. The Hamiltonian for the $N = N_\uparrow + N_\downarrow$ system is

$$H = \sum_i \left[\frac{p_i^2}{2m} + V_{\text{ext}}(x_i) \right] + g \sum_{i < j} \delta(x_i - x_j), \quad (1)$$

where m is the mass and the sums run over the number of particles, $i = 1, \dots, N$, x_i is the coordinate, and p_i the momentum of the i th particle. The external confinement, $V_{\text{ext}}(x)$, is assumed to be the same for all particles. Furthermore, we will assume that $V_{\text{ext}}(x)$ is parity invariant and has at least N bound states. The interaction strength g is positive for repulsive interactions and negative for attractive interactions. We note that since the parity operator commutes with the Hamiltonian, parity is conserved when g changes. While we only discuss the two-component Fermi system below, the case of bosons or Bose-Fermi mixtures is similar in spirit and in formalism and we return briefly to this extension in the outlook. For the majority of the discussion we assume all particles have equal mass, m , but we also discuss the important extension to mass-imbalanced systems. Notice that in the case of two-component Fermi systems, particles of the same spin projection will not interact due to the antisymmetry required by the Pauli principle which implies that the zero-range interaction will vanish for similar spin projections. For this reason we may use the general form of the Hamiltonian in Eq. (1) with the sum over $i < j$ also for fermionic systems.

Consider now an N -body system and assume that we have solved the problem for $g = 0$ with energy eigenstate $|\gamma_0\rangle$ and for $1/g = 0$ with eigenstate $|\gamma_\infty\rangle$. Now form the linear combination

$$|\gamma\rangle = \alpha_0 |\gamma_0\rangle + \alpha_\infty |\gamma_\infty\rangle. \quad (2)$$

This interpolatory ansatz is motivated by the intuitive idea that the wave function of a system with intermediate-strength interactions contains a mixture of qualities from the wave functions with weak and strong interactions. We may compute $\langle \gamma | H | \gamma \rangle$ as a function of α_0 and α_∞ and look for optimum values. As we shall demonstrate in this paper, $|\gamma\rangle$ provides a simple yet accurate description of the system for any value of g . The only exception is deeply bound states to which we return below.

We will demonstrate that the interpolatory ansatz in Eq. (2) can capture the qualitative features of the eigenstates of the Hamiltonian in Eq. (1) and is quantitatively accurate at the level of a few percent. Furthermore, we show that the expression for the optimum energy of $|\gamma\rangle$ may be modified slightly to make it perturbatively correct in both limits of the interaction strength. With this modification, the interpolatory ansatz provides an approximation to the eigenenergy with an accuracy that is comparable to state-of-the-art numerical methods, though the ansatz is far simpler.

We provide a proof of principle by considering some important examples from the few-body limit that are experimentally relevant at the moment. For this purpose we restrict to a harmonic confinement, i.e. $V_{\text{ext}}(x) = \frac{1}{2} m \omega^2 x^2$, throughout (here ω is the angular frequency of the oscillator).

The results we present here are

- Analytical expressions for the ansatz parameters α_0 and α_∞ that depend exclusively on two matrix elements in $|\gamma_0\rangle$ and $|\gamma_\infty\rangle$ (as well as the eigenenergies of these limiting states).
- The case $N = 2$ where one has the exact solution available³¹. Here we show that our method is accurate for both repulsive and attractive interactions to less than a few percent.
- The $N = 3$ case where no analytical solutions are known for general g . Here our ansatz provides very accurate results for all g . The results are compared to exact numerical diagonalisation utilising a unitary transformation of the interaction Hamiltonian.
- Energies for the impurity limit with $N_\downarrow = 1$ and $N_\uparrow = 1 - 5$ which we compare to experiments and find excellent agreement. We also discuss the Anderson orthogonality catastrophe for this system, which is related to the coefficient α_0 .
- An extension of the method to systems with particles of different mass. The examples we discuss are three-body systems and we compare to exact numerical results based on the correlated Gaussian method. This is the first application of the correlated Gaussian method to mass-imbalanced systems in 1D that we are aware of.

The ansatz we propose can be used to get very simple expressions for different observables as one needs to compute only a few matrix elements between the $g = 0$ and $1/g = 0$ states of interest. Our method is directly extendable to bosonic systems or mixed systems, as long as one has access to the two limiting wave functions, and while we have focused on harmonically confined systems it can be straightforwardly extended to any other form of confinement. Furthermore, one may systematically improve the ansatz by adding more states.

Results and Discussion

Let $|\gamma_0\rangle$ be an energy eigenstate in the non-interaction limit (that is, $g = 0$) with eigenenergy E_0 . We now adiabatically change the interaction strength from $g = 0$ to $|g| \rightarrow \infty$ and in turn we adiabatically change $|\gamma_0\rangle$ into a new state denoted $|\gamma_\infty\rangle$ with energy E_∞ . The wave function of the state $|\gamma_\infty\rangle$ vanishes whenever the position coordinates of any two particles coincide, and $|\gamma_\infty\rangle$ is thus unaffected by the interaction potential

$$V = g \sum_{i < j} \delta(x_i - x_j). \quad (3)$$

As our ansatz we now construct the trial state

$$|\gamma\rangle = \alpha_0 |\gamma_0\rangle + \alpha_\infty |\gamma_\infty\rangle, \quad (4)$$

where α_0 and α_∞ are real parameters. Assuming $|\gamma_0\rangle$ and $|\gamma_\infty\rangle$ are normalised, the energy of the trial state is

$$E = \frac{\langle \gamma | H | \gamma \rangle}{\langle \gamma | \gamma \rangle} = E_0 + \frac{\langle \gamma_0 | V | \gamma_0 \rangle \alpha_0^2 + \Delta E \alpha_\infty^2}{\alpha_0^2 + \alpha_\infty^2 + 2 \langle \gamma_0 | \gamma_\infty \rangle \alpha_0 \alpha_\infty}, \quad (5)$$

where we let $\Delta E \equiv E_\infty - E_0$.

We use a variational approach to solving the Schrödinger equation by identifying stationary points of the trial state energy functional Eq. (5). We thus select the values of α_0 and α_∞ that optimise the energy of the trial state for a given value of g . This will yield energies and eigenstates that, although approximate, turn out to be extremely accurate as discussed below.

Before presenting the results of the variational calculation, we shall briefly examine Eq. (5) in the limiting cases of the interaction strength: If we require that $\alpha_\infty/\alpha_0 \rightarrow 0$ for $g \rightarrow 0$ such that the trial state approaches $|\gamma_0\rangle$ in the non-interacting limit, Eq. (5) gives a first-order term in g of the form $\langle \gamma_0 | V | \gamma_0 \rangle$, in agreement with first order perturbation theory. We caution, however, that requiring $\alpha_0/\alpha_\infty \rightarrow 0$ (i.e. $|\gamma\rangle \rightarrow |\gamma_\infty\rangle$) for $1/g \rightarrow 0$, does not automatically ensure that the first order expansion of Eq. (5) in $1/g$ is equal to that of the exact eigenstate. We will come back to this point later on.

The coefficients that yield stationary points of Eq. (5) are given by (see the Supplementary Materials for details)

$$\left(\frac{\alpha_0}{\alpha_\infty} \right)_{\text{opt}}^{(\pm)} = \frac{\Delta E - \langle \gamma_0 | V | \gamma_0 \rangle \mp \sqrt{(\Delta E - \langle \gamma_0 | V | \gamma_0 \rangle)^2 + 4 \langle \gamma_0 | V | \gamma_0 \rangle \Delta E \langle \gamma_0 | \gamma_\infty \rangle^2}}{2 \langle \gamma_0 | V | \gamma_0 \rangle \langle \gamma_0 | \gamma_\infty \rangle}. \quad (6)$$

This gives the energy

$$E_{\text{opt}}^{(\pm)} = E_0 + \frac{\langle \gamma_0 | V | \gamma_0 \rangle + \Delta E \pm \sqrt{(\langle \gamma_0 | V | \gamma_0 \rangle + \Delta E)^2 - 4 \langle \gamma_0 | V | \gamma_0 \rangle \Delta E (1 - \langle \gamma_0 | \gamma_\infty \rangle^2)}}{2 (1 - \langle \gamma_0 | \gamma_\infty \rangle^2)}. \quad (7)$$

The denominator in Eq. (7) is positive because $|\langle \gamma_0 | \gamma_\infty \rangle| \leq 1$ by the Cauchy-Schwarz inequality. Hence, $E_{\text{opt}}^{(+)}$ is the energy maximum while $E_{\text{opt}}^{(-)}$ is the energy minimum. To ensure the correct energies in the limits $g = 0$ and $1/g = 0$, we use the energy minimum, $E_{\text{opt}}^{(-)}$, to approximate the eigenenergy whenever $g > 0$, while for $g < 0$ we use the energy maximum, $E_{\text{opt}}^{(+)}$.

While the interpolatory ansatz is extremely simple, it has a shortcoming in the $1/g \rightarrow 0$ limit where it does not reproduce the slope of the energy. As is shown in the following, we may, however, modify the ansatz slightly to correct this behaviour. Letting $q \equiv -1/g$, the first-order expansion $E_{\text{opt}} = E_\infty + K_{\text{opt}}^\infty q$ has the slope

$$K_{\text{opt}}^\infty = \left. \frac{\partial E_{\text{opt}}}{\partial q} \right|_{q=0} = \frac{\Delta E^2}{K^0} \langle \gamma_0 | \gamma_\infty \rangle^2, \quad (8)$$

where $K^0 = \langle \gamma_0 | V | \gamma_0 \rangle / g$ is the corresponding slope of the energy curve in the limit of vanishing interactions. This demonstrates that the important quantity in the slope is the overlap $\langle \gamma_0 | \gamma_\infty \rangle$. In the original philosophy of the ansatz, we exploit that we know both wave functions in this overlap exactly and thus also the overlap itself; this leaves no unfixed parameters. Realising that this yields a discrepancy we have explored how to modify this assumption in order to improve the approximation.

To this end, we note that the derivation of Eq. (7) actually does not depend on $|\gamma_\infty\rangle$ being an energy eigenstate. It must be a state with energy E_∞ (with respect to the non-interacting Hamiltonian), but beyond that the only requirement of $|\gamma_\infty\rangle$ is that $V|\gamma_\infty\rangle = 0$. Furthermore, E_{opt} only depends on $|\gamma_\infty\rangle$ through the squared wave-function overlap $\langle \gamma_0 | \gamma_\infty \rangle^2$. Thus, if we substitute

$\langle \gamma_0 | \gamma_\infty \rangle^2$ in Eqs. (7)–(8) with some parameter λ , we may regard E_{opt} and K_{opt}^∞ as functions of λ . We can then select λ such that $E_{\text{opt}}(\lambda)$ becomes perturbatively correct, that is $K_{\text{opt}}^\infty(\lambda) = K_{\text{exact}}^\infty$, or,

$$\lambda = \frac{K^0 K_{\text{exact}}^\infty}{\Delta E^2}, \quad (9)$$

where K_{exact}^∞ is the slope of the true eigenenergy curve at $q = 0$ (which is known exactly using the formalism of A.G.V. *et al.*²²). We shall refer to this perturbatively correct modification, $E_{\text{opt}}(\lambda)$, as the *modified ansatz*. Note that this modification breaks variational bounds since we have no *a priori* knowledge of any trial state whose energy is $E_{\text{opt}}(\lambda)$. By going from the original interpolatory ansatz to the modified ansatz, we lose information about the wave function, but gain the correct slope of the energy at $1/g \rightarrow 0$. Below we will see that the modified ansatz increases the accuracy significantly as compared to the original ansatz.

We now proceed to discuss examples of the ansatz. Throughout our discussion, the external potential is taken to be harmonic $V_{\text{ext}}(x) = \frac{1}{2} \omega^2 m x^2$ and the same for all particles. This is the most widely studied and experimentally relevant case at the moment so it will be our focus here. Henceforth, we use natural units $\hbar = m = \omega = 1$ such that energies are given in units of $\hbar\omega$, lengths in units of $\sigma = \sqrt{\hbar/m\omega}$, and interaction strengths g in units of $\sigma\hbar\omega$.

Two particles

The $N = 2$ case is special as analytical results for any g are available due to the seminal work of Busch *et al.*³¹. It is therefore an important benchmark case for our approach. First we note that we will only be interested in the relative energy as the center of mass decouples in the harmonic trap. Note that this decoupling is not an essential assumption of our method and is merely a convenience.

The details on how to construct the ansatz states for the two-particle case are given in the Methods section below. The energy spectrum using the interpolatory ansatz of Eq. (7) is shown in Fig. 1. Only the even-parity solutions are shown on the plot as odd-parity states are unchanged by the zero-range interaction. The figure also includes experimental measurements of the ground-state energy. The experiment has been conducted by S. Jochim's ultra-cold atoms group in Heidelberg, and the data originates from Wenz *et al.*¹⁹. This data has been corrected for the imperfections of the trap as described in Wenz *et al.*¹⁹. As seen, the experimental data agrees with the interpolatory ansatz well within the experimental uncertainties.

If we expand the energy in terms of g , the first-order term agrees with the result of ordinary non-degenerate perturbation theory. Similarly, in the limit $1/g = 0$, the energy curve (as a function of q) of the true eigenstate has the same slope as that of our interpolatory ansatz.

The inset in Fig. 1 shows a zoom of the energy spectrum on the ground state and compares the energy predicted by Eq. (7) with the exact solution. For $q > 0$ the energy of the interpolatory ansatz is within 0.05 of the exact energy in the vicinity of $q \sim 0.4$ and even less elsewhere. The error decreases as we move up in the spectrum. For $q < 0$ the deviation is less than 0.006 for the ground state; again greatest around $q \sim -0.4$. On this side, the error increases for the excited states, but we find that it is bounded by about 0.03.

We conclude that the ansatz is extremely accurate for the $N = 2$ case where we can compare to analytical results³¹. One may also compare the wave functions and again find extremely good agreement (see Supplementary Fig. S1 online).

For attractive interactions, a deeply bound molecular state exists that we have so far ignored. However, it turns out that the ansatz of Eq. (7) can be extended to also give extremely accurate results for the deeply bound state. As is shown in the Supplementary Materials, this can be done by including an additional state in the ansatz that has the correct asymptotic behaviour as $g \rightarrow -\infty$. We stress that this is in fact in complete agreement with the universal philosophy of the ansatz method, i.e. interpolation between (known) extremes. Thus to address deeply bound states one needs a state in the extreme limit of large negative energy. This yields a very precise approximation also for the deeply bound state. This highlights the universal nature of our approach. We will not pursue the deeply bound states any further in this paper.

Three particles

The simplest non-trivial example of a three-body two-component Fermi system has $N_\uparrow = 2$ and $N_\downarrow = 1$. The interaction potential is

$$V = g(\delta(x_1 - x_2) + \delta(x_1 - x_3) + \delta(x_2 - x_3)), \quad (10)$$

and we let x_1 be the position of the spin-down fermion, while x_2 and x_3 denote the position of spin-up fermions. Again the third interaction term will vanish for identical fermions but we keep it for generality.

Eigenstates of the harmonic Hamiltonian are described by two quantum numbers, $\nu \geq 0$ and $\mu \geq 1$, which we shall call the radial quantum number and the angular quantum number, respectively. The eigenenergies are

$$E_{\nu,\mu} = 2\nu + \mu + 1. \quad (11)$$

The quantum numbers ν and μ can be used to describe the energy eigenstates in both the non-interacting limit and the infinite-interaction limit.

Constructing the ansatz

Recall that $|\gamma_0\rangle$ and $|\gamma_\infty\rangle$ denote eigenstates in the non-interacting limit and the infinite-interaction limit, respectively, and that we are looking for states that are adiabatically connected. As states with different radial quantum number ν are orthogonal, we assume that the adiabatically connected states have the same ν values. Parity p is exactly conserved and thus also the same for two states in the ansatz. The quantity that changes with g is therefore the μ quantum number, and we call the limiting values μ_0 and μ_∞ , respectively. The angular quantum numbers are related by

$$|\Delta\mu| = |\mu_\infty - \mu_0| = \frac{3 + (-1)^{\mu_\infty} p}{2}. \quad (12)$$

For repulsive interactions, $\mu_0 < \mu_\infty$, and for attractive interactions, $\mu_0 > \mu_\infty$, cf. Eq. (11). The optimum energy of the trial state can now be determined using Eq. (7) with E_0 and E_∞ given by Eq. (11).

Energy spectrum

Figure 2 shows the energy spectrum for $E < 8$ (deeply bound states are not considered) both as calculated using the interpolatory ansatz and by exact numerical diagonalisation. The interpolatory ansatz clearly describes the qualitative features of the spectrum well; both for repulsive and attractive interactions. In this energy-range, the $\nu = 0$ states also give a good quantitative match to the numerical results. However, the error seems to grow with ν .

We see in Fig. 2 that trial states with $\nu = 0$ and $\Delta\mu = 1$ offer a particularly good approximation to the corresponding eigenstates in the repulsive region (see e.g., the first excited state). This is because the slope of the energy curve, that is $K_{\text{opt}}^\infty = \partial E_{\text{opt}}^{(-)} / \partial q$, at $q = 0$ is the same as that of the exact eigenenergy. For the trial states with $\Delta\mu = 2$, this is generally not the case. This result suggests that K_{opt}^∞ is an important quantity to reproduce correctly in an attempt such as the present to describe the physics of our problem through a simple ansatz. Note also, that the slope of the energy curve has a discontinuity at $1/g = 0$, which contradicts the expectation that the states go smoothly through this region.

If we now enforce the correct slope by a modification of the interpolatory ansatz as proposed in the discussion following Eq. (8), we arrive at the spectrum shown in Fig. 3. We see that the modified ansatz agrees better with the numerical results than the original ansatz; especially for states with $\nu > 0$. There are, however, still deviations on the attractive side of the spectrum, and for high energies, also on the repulsive side. We shall give a quantitative discussion of the quality of the approximation when discussing the impurity system below. We have included the experimental measurements of the ground-state energy¹⁹ in the figure and see that both ansatz and modified ansatz agrees very nicely with experiment, although for large g the modified ansatz naturally does better.

Mass-imbalanced systems

In the case of different masses, one typically uses another length scale given by $\sigma = \sqrt{\hbar/\eta\omega}$ where $\eta = \sqrt{m_1 m_2 m_3 / (m_1 + m_2 + m_3)}$, and m_1 is the mass of the spin-down fermion while m_2 and m_3 are the masses of the spin-up fermions. We now consider the case where $m_1 = M$ and $m_2 = m_3 = m$.

In Fig. 4 we show the energy spectrum obtained by the interpolatory ansatz for $M/m = 1/2$ and $M/m = 2$ and compare this with numerically calculated results using the correlated Gaussian approach (see the Supplementary Materials for details on the numerical methods). The agreement between the ansatz and the numerical results is striking for the low-energy part of the spectrum considered here, and we see that the ansatz can be extended also to mass-imbalanced systems.

Impurity systems

We now consider a system of N fermions among which one particle (x_1) is spin-down and the $N_\uparrow = N - 1$ remaining particles (x_2, \dots, x_N) are spin-up. Taking into account that interactions between identical fermions vanish, we can write the interaction term as

$$V = g \sum_{k=2}^N \delta(x_1 - x_k). \quad (13)$$

We restrict the discussion to the ground state with repulsive interactions as this has been a focus of recent experimental attention¹⁹. The considerations can be extended to obtain more states in the spectrum, to the attractive side, and to deeply bound states in the same manner as in the previous examples.

We denote by $|\gamma_\Lambda\rangle$ the Slater determinant of the single-particle harmonic eigenstates $\langle x_k | n \rangle = \psi_n(x_k)$ for $k = 1, \dots, N$ and $n = 0, \dots, N - 1$. Here $\psi_n(x)$ is the single-particle eigenstate of the harmonic oscillator Hamiltonian in coordinate space with

quantum number n and argument x . The state $|\gamma_A\rangle$ is antisymmetric with respect to interchange of any two coordinates, so $\langle\gamma_A|V|\gamma_A\rangle = 0$. We can write the antisymmetric state as

$$|\gamma_A\rangle = \sum_{k=1}^N |\gamma_A\rangle_k, \quad (14)$$

if we define

$$|\gamma_A\rangle_k \equiv \sum_{\substack{\sigma \in S_N \\ \sigma(1)=k}} \int_{\Pi(\sigma)} d\mathbf{x} |\mathbf{x}\rangle \langle \mathbf{x} | \gamma_A \rangle, \quad (15)$$

where $\mathbf{x} = (x_1, \dots, x_N)$, S_N is the symmetric group of order N , and $\Pi(\sigma)$ indicates the integration region $x_{\sigma(1)} < \dots < x_{\sigma(N)}$. In each region, $\Pi(\sigma)$, the wave function of the ground state in the infinite-interaction limit is proportional to $\langle \mathbf{x} | \gamma_A \rangle$. The (normalised) ground state in the infinite-interaction limit is then

$$|\gamma_\infty\rangle = \sqrt{\frac{N}{\sum_{i=1}^N a_i^2}} \sum_{k=1}^N a_k |\gamma_A\rangle_k \quad (16)$$

for some coefficients $\mathbf{a} = (a_1, \dots, a_N)$ to be determined by the method of A.G.V. *et al.*²² (see the Supplementary Materials). The ground state in the non-interaction limit is the single-particle harmonic eigenstate $\psi_0(x_1)$ multiplied by the Slater determinant for the remaining particles in the states $\psi_n(x_k)$ for $k = 2, \dots, N$ and $n = 0, \dots, N-2$.

For systems of four and five particles, the interpolatory ansatz with these $|\gamma_0\rangle$ and $|\gamma_\infty\rangle$ yields integrals that can be evaluated analytically. For larger systems, the integrals are readily evaluated numerically. The resulting energies for $N = 4-6$ are plotted as dashed lines in Fig. 5. Here we see a very good agreement between the ansatz and the numerically exact results, and in turn excellent agreement with experimental measurements¹⁹. This indicates that the energetics of the system is captured by the interpolatory ansatz with high accuracy.

However, as we discussed briefly above, the ansatz does not generally reproduce the correct first-order energy term at $1/g = 0$. Assuming that the non-interacting state should remain untouched, this prompts us to investigate whether another state can be found in the $1/g = 0$ limit that can replace $|\gamma_\infty\rangle$ in Eq. (4) and in turn give the exact result for the slope of the energy at $1/g = 0$. As noted above, Eq. (7) remains valid if we substitute the eigenstate $|\gamma_\infty\rangle$ with any other state with energy E_∞ that obeys $V|\gamma_\infty\rangle = 0$. In particular, any choice of \mathbf{a} in Eq. (16) would work, and E_{opt} only depends on \mathbf{a} through the wave-function overlap $\langle \gamma_0 | \gamma_\infty \rangle$. Hence, because E_{opt} is monotonic in $\langle \gamma_0 | \gamma_\infty \rangle^2$, we may optimise the energy with respect to \mathbf{a} for all values of g by maximising $\langle \gamma_0 | \gamma_\infty(\mathbf{a}) \rangle^2$ with respect to \mathbf{a} . Leaving the details to the Supplementary Materials, the optimum is

$$\langle \gamma_0 | \gamma_\infty(\mathbf{a}_{\text{max}}) \rangle^2 = N \sum_{m=1}^N \langle \gamma_0 | \gamma_A \rangle_m^2 \quad (17)$$

with

$$\mathbf{a}_{\text{max}} \propto (\langle \gamma_0 | \gamma_A \rangle_1, \langle \gamma_0 | \gamma_A \rangle_2, \dots, \langle \gamma_0 | \gamma_A \rangle_N). \quad (18)$$

For the ground state of the $N = 3-6$ systems, however, $\langle \gamma_0 | \gamma_\infty(\mathbf{a}_{\text{max}}) \rangle^2$ is very close to the known exact value of $\langle \gamma_0 | \gamma_\infty \rangle^2$, and is not large enough to make the slope of the energy correct in the strongly-interacting limit, that is, $\langle \gamma_0 | \gamma_\infty(\mathbf{a}_{\text{max}}) \rangle^2 < \lambda$ with λ given by Eq. (9). This indicates that we cannot find a state in the infinite-interaction limit that both has the correct zeroth-order energy, E_∞ , and satisfies the delta-boundary conditions, $V|\gamma_\infty\rangle = 0$. However, we caution that this is under the assumptions that the wave function of $|\gamma_\infty\rangle$ is continuous and has discontinuous derivatives that satisfy the boundary conditions imposed by the zero-range interaction.

We see that the interpolatory ansatz – with whatever choice of $|\gamma_\infty\rangle$ – does not reproduce the correct energy slope. The modified ansatz, however, does. It is worthwhile to note that the inability to find a state, $|\gamma\rangle = \alpha_0 |\gamma_0\rangle + \alpha_\infty |\gamma_\infty\rangle$, whose expectation value is that predicted by the modified ansatz, does not imply that the modified ansatz cannot be used. The two methods rely on different information about the system: The interpolatory ansatz requires the knowledge of the wave function at $g = 0$ and $1/g = 0$, whereas the modified ansatz uses the knowledge of the energy behaviour. Therefore, one can use the modified ansatz to estimate the energies, and the interpolatory ansatz to approximate the wave functions.

Figure 5 compares the ground-state energy of the modified ansatz with results from an exact numerical diagonalisation as well as experimental data¹⁹. Here we see an improved agreement for large g . The deviations of the modified ansatz from exact numerical diagonalisation are shown in greater detail in Figure 6. The errors are more than an order of magnitude smaller than those of the unmodified ansatz (shown in Supplementary Fig. S4 online).

We plot the error scaled against N_{\uparrow} instead of E_0 or E , because E_0 scales as N_{\uparrow}^2 while $\Delta E = N_{\uparrow}$. As seen in Fig. 5, the maximum in the error moves to larger interaction strength for higher N_{\uparrow} , i.e. with system size. There seems to be only very little increase in the magnitude of the error for larger N_{\uparrow} for the system sizes we have studied. Notice that the error is slightly negative for $1/g \simeq 0$ in the cases $N = 3 - 6$. Since we know the exact energies and slopes around $1/g = 0$, the likely cause of this is that we are pushing the accuracy of the exact numerical diagonalisation method here.

Our first observation is that the approximation of the ground-state energy offered by the modified ansatz is so good that it can compete and even in some cases beat state-of-the-art numerical exact methods. The drawback seems quite evident, i.e. we cannot be sure that any state exists in the infinite-interaction limit that when used in Eq. (5) would reproduce the energy of the modified ansatz. Thus, the modified ansatz does not immediately give us any information about the wave function in spite of its near perfect approximation of the energy. We also note that the modified ansatz breaks the variational bound on the ground state and can in principle have lower energy as compared to the exact result. However, we have clearly demonstrated that the slope of the energy at $1/g = 0$ is an extremely important quantity for these systems as it appears crucial to reproduce in order to capture the energetics. This highlights the important role played by the recently developed theory of strongly interacting confined systems²².

Anderson overlap

Finally, we discuss the so-called Anderson overlap, which is the wave-function overlap between the non-interacting eigenstate, $|\gamma_0\rangle$, and the interacting state, $|\gamma\rangle$, for some value of the interaction strength, g . This quantity is related to the Anderson orthogonality catastrophe³², which states that the Anderson overlap is zero in the thermodynamic limit; that is $\langle\gamma_0|\gamma\rangle \rightarrow 0$ for $N \rightarrow \infty$, and in particular $\langle\gamma_0|\gamma_{\infty}\rangle \rightarrow 0$ for $N \rightarrow \infty$.

In Fig. 7 we illustrate how the overlap $\langle\gamma_0|\gamma\rangle^2$ – with $|\gamma\rangle$ given by the interpolatory ansatz – decreases as a function of g . Due to the fact that we only consider a finite-sized system, the overlap does not approach zero as $g \rightarrow \infty$, but the plot clearly shows that the overlap from our interpolatory ansatz tends to decrease as expected. The fact that the ansatz gives a very accurate approximation for the energy of the system does not immediately imply that this is also the case for the wave function. We leave this question for future studies, and the overlaps presented here are thus predictions based on the ansatz. It should be compared either to elaborate exact numerical calculations or to experimental measurements.

Outlook

We have proposed a simple interpolatory ansatz for approximating the energy eigenstate of a confined, one-dimensional system of interacting particles. The ansatz is a linear combination of known eigenstates in the extreme limits of the interaction strength, $g \rightarrow 0$ and $1/g \rightarrow 0$, respectively. Thanks to recent advances in the description of the eigenstates in the $1/g = 0$ limit, both these wave functions are now available. An analytical expression for the optimum energy of this ansatz is presented which is an elementary function of only two matrix elements; the interaction energy of the eigenstate at $g = 0$, and the wave-function overlap between the eigenstates in the two limits of $g \rightarrow 0$ and $1/g \rightarrow 0$. By focusing on harmonically trapped impurity systems of fermions, we have demonstrated that the ansatz is able to capture the physics of such a system. It gives us a highly accurate approximation for the energy and it also gives us a very simple expression for the wave function.

For both the two- and three-particle systems, we have been able to reproduce the entire energy spectrum with the interpolatory ansatz, save for deeply bound molecular states. The ansatz can be extended to describe deeply bound states as well; this has been shown specifically for the two-particle system. Taking the three-particle system as an example, we have also demonstrated that the ansatz works equally well for mass-imbalanced systems. A future extension of this study might investigate mass-imbalanced systems of four or more particles. It should be noted that the bottleneck here is that there are generally quite few known results about mass-imbalanced systems in the $1/g \rightarrow 0$ limit³³. It is an open problem to find a general method that yields exact eigenstates in the strongly interacting regime for mass-imbalanced systems.

A drawback of our ansatz is that it is in general not perturbatively correct in the strongly-interacting regime. More precisely, if we take the first order derivative of the energy with respect to $1/g$ it deviates from the known exact result. We may, however, modify the expression for the energy of the interpolatory ansatz slightly such that it is perturbatively correct to linear order in g for $g \rightarrow 0$ and to linear order in $1/g$ for $1/g \rightarrow 0$. The modified ansatz has great simplicity and accuracy at a level that is competitive with state-of-the-art numerical methods for obtaining the energy of the ground state for arbitrary g . Due to its simplicity it should provide a very useful tool.

We note that although the results presented here assume that the particles are trapped in an external harmonic trap, the formalism is completely general and can be applied for arbitrary external potentials with at least N bound single-particle states for N -body systems. As we have shown, the relative deviation of the energy obtained from the ansatz grows only very slowly with N , and there should be no problem in extending the technique to even larger systems than considered here. The decisive quantity is the overlap of the $g = 0$ and $1/g = 0$ wave functions. This overlap may be computed using the same methods that

have recently been used to compute spin chain models for strongly interacting fermions³⁴ and thus scaling to larger N of order 30 or 40 is certainly within reach.

A future direction would be to consider a generalised version of the interpolatory ansatz where one systematically adds more states at $g = 0$ and $1/g = 0$ in order to gradually improve the comparison. In addition, it is relatively straightforward to apply the interpolatory ansatz in the case of strongly interacting bosons^{35,36}, or mixed systems^{22,28}. The requirements are knowledge of states in the two limits and their overlaps so that the interpolation can be performed. The formulae for the interpolated energy given here still apply. An example could be an impurity interacting strongly with a Tonks-Girardeau gas of hard-core bosons, which is a topic of great recent interest^{37–39}.

Methods

In the following, we provide the details of the methods used in applying the interpolatory ansatz to two-, three- and many-particle systems.

Details of the two-particle system

We consider a system of two distinguishable fermions and we define $x = (x_1 - x_2)/\sqrt{2}$. In the absence of interactions, the energy eigenstates are the harmonic eigenstates denoted $|n\rangle$ with integer $n \geq 0$ (we are only concerned with the motion relative to the center of mass).

Exact solutions of the two-particle problem are available for arbitrary values of g ^{31,40}. The energy of an exact energy eigenstate is given indirectly by⁴⁰

$$q = \frac{1}{2\sqrt{2}} \frac{\Gamma(\frac{1-2E}{4})}{\Gamma(\frac{3-2E}{4})}, \quad (19)$$

and the wave function of the state is

$$\psi(x) = \left(-\sqrt{2}q {}_1F_1\left(\frac{1-2E}{4}; \frac{1}{2}; x^2\right) + |x| {}_1F_1\left(\frac{3-2E}{4}; \frac{3}{2}; x^2\right) \right) e^{-x^2/2} \quad (20)$$

where ${}_1F_1$ is the confluent hypergeometric function of the first kind.

Constructing the ansatz

Let $|\gamma_0\rangle = |n_1\rangle$ be an energy eigenstate in the non-interaction limit. Here $|n_1\rangle$ is a single-particle eigenstate of a harmonic oscillator Hamiltonian (in the relative coordinate x) with quantum number n_1 . Furthermore, let $|\gamma_\infty\rangle$ be the corresponding eigenstate in the infinite-interaction limit – that is, $|\gamma_0\rangle \rightarrow |\gamma_\infty\rangle$ as the interaction strength is changed adiabatically from $g = 0$ to $1/g = 0$. By conservation of parity, the states $|\gamma_0\rangle$ and $|\gamma_\infty\rangle$ have the same parity.

If $|\gamma_0\rangle$ is odd, $\langle x = 0 | \gamma_0 \rangle = 0$ and thus $\langle \gamma_0 | V | \gamma_0 \rangle = 0$. Hence, odd harmonic eigenstates do not change as we introduce a non-zero interaction. The even harmonic eigenstates do, however, change; the correct even eigenstate in the infinite-interaction limit is

$$|\gamma_\infty\rangle = \int dx |x\rangle \text{sgn}(x) \langle x | n_2 \rangle \quad (21)$$

with $n_2 = n_1 + 1$ for repulsive interactions ($g > 0$) and $n_2 = n_1 - 1$ for attractive interactions ($g < 0$).

Details of the three-particle system

Before we employ the interpolatory ansatz, we first separate out the center-of-mass motion using hyperspherical coordinates^{35,41}. This is done merely for convenience and is not in any way essential for the approach. Defining $x = (x_2 - x_3)/\sqrt{2}$ and $y = (x_2 + x_3)/\sqrt{6} - 2x_1/\sqrt{6}$, the hyperradius is given by $\rho = \sqrt{x^2 + y^2}$ and the hyperangle is defined by $\tan \phi = y/x$. The Hamiltonian of the relative motion becomes

$$H = \frac{1}{2}(\nabla^2 + \rho^2) + V, \quad (22)$$

where ∇^2 is the Laplacian in polar coordinates (ρ, ϕ) and

$$V = \frac{g}{\sqrt{2}\rho} \sum_{j=1}^6 \delta\left(\phi - \frac{2j-1}{6}\pi\right) \quad (23)$$

is the interaction.

Limiting cases

The quantum numbers ν and μ can be used to describe the energy eigenstates in both the non-interacting limit and the infinite-interaction limit. The eigenstate wave function in both limits has the general form⁴¹

$$\Psi_{\nu,\mu}(\rho, \phi) = \sqrt{\frac{2\nu!}{(\nu+\mu)!}} L_{\nu}^{\mu}(\rho^2) e^{-\rho^2/2} \rho^{\mu} \Phi_{\mu}(\phi), \quad (24)$$

where L_{ν}^{μ} is a generalised Laguerre polynomial.

In the non-interacting limit, the (normalised) angular part of the wave function is

$$\Phi_{\mu}(\phi) = \frac{1}{\sqrt{\pi}} \cdot \begin{cases} \cos(\mu\phi), & \text{for } p = -1 \\ \sin(\mu\phi), & \text{for } p = +1, \end{cases} \quad (25)$$

where p is the parity of the wave function. In this limit $p = (-1)^{\mu}$.

In the infinite-interaction limit, the wave function vanishes at the lines $\phi = -5\pi/6, -\pi/2, -\pi/6, \pi/6, \pi/2, 5\pi/6$. In the regions between these lines, the wave function solves the Schrödinger wave equation for the harmonic oscillator without interactions.

The eigenenergies in the limit $1/g = 0$ is given by Eq. (11) with $\mu = 3, 6, 9, 12, \dots$. Each allowed eigenenergy is three-fold degenerate (not counting states with a different radial quantum number ν): One of the eigenstates in each energy triplet is a harmonic eigenstate with $\mu = 3, 6, 9, 12, \dots$ which is unaffected by the interactions. Between the two remaining eigenstates in the triplet, one is odd and the other is even.

When μ is even (that is, $\mu = 6, 12, 18, \dots$) the non-trivial eigenstates in the infinite-interaction limit have the angular wave function

$$\Phi_{\mu}(\phi) = \sqrt{\frac{2-p}{2\pi}} \sin(\mu\phi) \cdot \begin{cases} -p-1, & \text{for } -\frac{\pi}{6} \leq \phi < \frac{\pi}{6} \\ 1, & \text{for } \frac{\pi}{6} \leq \phi < \frac{\pi}{2}, \end{cases} \quad (26)$$

if p is their parity. The coefficients in the four remaining regions follow by symmetry considerations.

When μ is odd ($\mu = 3, 9, 15, \dots$),

$$\Phi_{\mu}(\phi) = \sqrt{\frac{2+p}{2\pi}} \cos(\mu\phi) \cdot \begin{cases} p-1, & \text{for } -\frac{\pi}{6} \leq \phi < \frac{\pi}{6} \\ 1, & \text{for } \frac{\pi}{6} \leq \phi < \frac{\pi}{2}. \end{cases} \quad (27)$$

Details of the mass-imbalanced system

The transformation into hyperspherical coordinates proceeds along the same lines with a modified Jacobian. Generally, the coordinates $\mathbf{x} = (x_1, x_2, x_3)$ are transformed to Jacobi coordinates, $\mathbf{x}' = \mathbf{J}\mathbf{x}$, through the transformation matrix

$$\mathbf{J} = \frac{1}{\sqrt{\mu}} \begin{bmatrix} 0 & \frac{\mu_{23}}{\mu m_2} & \frac{-\mu_{23}}{\mu m_3} \\ -\frac{\mu_{23}}{m_1} & \frac{\mu_{23} M_{23}}{m_2} & \frac{\mu_{23} M_{23}}{m_3} \\ \frac{1}{\sqrt{M_{123}}} & \frac{1}{\sqrt{M_{123}}} & \frac{1}{\sqrt{M_{123}}} \end{bmatrix}, \quad (28)$$

where $M_{23} = m_2 + m_3$, $M_{123} = m_1 + m_2 + m_3$ and the ‘reduced’ masses are defined as $\mu_{23} = \sqrt{m_2 m_3 / M_{23}}$ and $\mu = \sqrt{m_1 m_2 m_3 / M_{123}}$. This transformation allows us to separate the center-of-mass motion from the relative motion, the solutions of the former being the well-known harmonic eigenstates. Afterwards, we transform the remaining relative coordinates into hyperspherical coordinates, ρ and ϕ , by $\rho = \sqrt{x_1'^2 + x_2'^2}$ and $\tan(\phi) = x_2'/x_1'$.

From now on, we assume that $m_1 = M$ and $m_1 = m_2 = m$. The interaction potential can then be written as

$$V = \frac{g}{\rho} \sqrt{\frac{2\zeta}{\zeta^2 + 1}} \left(\sum_{\pm} \delta(\phi \pm \theta_0) + \delta(\phi \pm \theta_0 - \pi) \right), \quad (29)$$

where $\theta_0 = \arctan(\zeta)$ and $\zeta \equiv \mu/m = \sqrt{M/(2m+M)}$. As for the equal-mass case, the energy is given by Eq. (11)⁴².

The μ eigenvalue can be found by using parity symmetry, the Pauli principle and the delta-boundary conditions of the interaction potential. Using these conditions, one can setup an equation from which μ can be obtained in the limits $g = 0$ and $1/g = 0$: For solutions with odd parity, μ solves the equation

$$\cos(\mu\pi/2) + \frac{\rho g}{\mu} \sqrt{\frac{8\zeta}{\zeta^2 + 1}} \sin(\mu(\pi/2 - \theta_0)) \cos(\mu\theta_0) = 0. \quad (30)$$

For even-parity solutions, the equation is

$$\sin(\mu\pi/2) + \frac{\rho g}{\mu} \sqrt{\frac{8\zeta}{\zeta^2 + 1}} \sin(\mu(\pi/2 - \theta_0)) \sin(\mu\theta_0) = 0. \quad (31)$$

Once μ is found, the wave function is also known cf. Eq. (24) and the energy is given by Eq. (11)⁴².

The wave function in the infinite-interaction limit now vanishes along the delta-boundary lines $\phi = \pm\theta_0, \pm\pi/2, \pi \pm \theta_0$. Only when $M = m$, is the wave function non-zero in all six regions separated by the delta-boundary lines. In order to illustrate this, we look at two explicit examples where $M/m = 1/2$ and $M/m = 2$, respectively. For the case of $M/m = 1/2$, we have $\theta_0 \simeq 0.421$ (or 24.1°), and the lowest-energy solutions of Eqs. (30)–(31) at $1/g = 0$ have $\mu \simeq 0.731$ (both odd and even) while the second-lowest has $\mu \simeq 3.735$ (odd). The angular part of the wave function for the ground state and the first excited state in the infinite-interaction limit are

$$\Phi_\mu^{(\mp)}(\phi) = \begin{cases} \mp \sin(\mu(\phi + \theta_0)), & \text{for } \phi \in [-\frac{\pi}{2}, -\theta_0] \\ 0, & \text{for } \phi \in [-\theta_0, \theta_0] \\ \sin(\mu(\phi - \theta_0)), & \text{for } \phi \in [\theta_0, \frac{\pi}{2}], \end{cases} \quad (32)$$

where \mp is the parity of the state. The angular part for the non-degenerate second excited state is

$$\Phi_\mu^{(-)}(\phi) = \begin{cases} 0, & \text{for } \phi \in [-\frac{\pi}{2}, -\theta_0] \\ \cos(\mu\phi), & \text{for } \phi \in [-\theta_0, \theta_0] \\ 0, & \text{for } \phi \in [\theta_0, \frac{\pi}{2}]. \end{cases} \quad (33)$$

When $M/m = 2$, the roles are reversed. The ground state is now non-degenerate with $\mu \simeq 2.552$ at $g = \infty$ and $\theta_0 \simeq 0.615$ (or 35.2°). In addition, the wave function has the same form as Eq. (33), only with different θ_0 and μ . For the first and second excited states, the wave function has the form of Eq. (32).

One might think that there would be some continuous crossover from $M < m$ to $M = m$ and then to $M > m$, but this is not the case. Indeed, $M = m$ is a singular case where the wave function is non-zero in all six regions.

References

1. Giamarchi, T. *Quantum Physics in One Dimension* (Oxford University Press Inc., New York, 2003).
2. Bezryadin, A. *Superconductivity in Nanowires* (WILEY-VCH Verlag, Weinheim, Germany, 2013).
3. Altomare, F. & Chang, A. M. *One-Dimensional Superconductivity in Nanowires* (WILEY-VCH Verlag, Weinheim, Germany, 2013).
4. Anderson, P. W. The resonating valence bond state in La_2CuO_4 and superconductivity. *Science* **235**, 1196–1198 (1987).
5. Lee, P. A., Nagaosa, N. & Wen, X.-G. Doping a mott insulator: Physics of high-temperature superconductivity. *Rev. Mod. Phys.* **78**, 17–85 (2006).
6. Lewenstein, M. *et al.* Ultracold atomic gases in optical lattices: mimicking condensed matter physics and beyond. *Advances in Physics* **56**, 243–379 (2007).
7. Bloch, I., Dalibard, J. & Zwerger, W. Many-body physics with ultracold gases. *Rev. Mod. Phys.* **80**, 885–964 (2008).
8. Moritz, H., Stöferle, T., Köhl, M. & Esslinger, T. Exciting collective oscillations in a trapped 1D gas. *Phys. Rev. Lett.* **91**, 250402 (2003).
9. Stöferle, T., Moritz, H., Schori, C., Köhl, M. & Esslinger, T. Transition from a strongly interacting 1D superfluid to a Mott insulator. *Phys. Rev. Lett.* **92**, 130403 (2004).
10. Kinoshita, T., Wenger, T. & Weiss, D. S. Observation of a one-dimensional Tonks-Girardeau gas. *Science* **305**, 1125–1128 (2004).
11. Paredes, B. *et al.* Tonks-Girardeau gas of ultracold atoms in an optical lattice. *Nature* **429**, 277–281 (2004).
12. Kinoshita, T., Wenger, T. & Weiss, D. S. A quantum Newton’s cradle. *Nature* **440**, 900–903 (2006).
13. Haller, E. *et al.* Realization of an excited, strongly correlated quantum gas phase. *Science* **325**, 1224–1227 (2009).
14. Haller, E. *et al.* Pinning quantum phase transition for a luttinger liquid of strongly interacting bosons. *Nature* **466**, 597–600 (2010).

15. Pagano, G. *et al.* A one-dimensional liquid of fermions with tunable spin. *Nat Phys* **10**, 198–201 (2014). Letter.
16. Serwane, F. *et al.* Deterministic preparation of a tunable few-fermion system. *Science* **332**, 336–338 (2011).
17. Zürn, G. *et al.* Fermionization of two distinguishable fermions. *Phys. Rev. Lett.* **108**, 075303 (2012).
18. Zürn, G. *et al.* Pairing in few-fermion systems with attractive interactions. *Phys. Rev. Lett.* **111**, 175302 (2013).
19. Wenz, A. N. *et al.* From few to many: Observing the formation of a Fermi sea one atom at a time. *Science* **342**, 457–460 (2013).
20. Murmann, S. *et al.* Two fermions in a double well: Exploring a fundamental building block of the Hubbard model. *Phys. Rev. Lett.* **114**, 080402 (2015).
21. Murmann, S. *et al.* Antiferromagnetic Heisenberg spin chain of a few cold atoms in a one-dimensional trap. *Phys. Rev. Lett.* **115**, 215301 (2015).
22. Volosniev, A. G., Fedorov, D. V., Jensen, A. S., Valiente, M. & Zinner, N. T. Strongly interacting confined quantum systems in one dimension. *Nat Commun* **5** (2014). Article.
23. Cui, X. & Ho, T.-L. Ground-state ferromagnetic transition in strongly repulsive one-dimensional Fermi gases. *Phys. Rev. A* **89**, 023611 (2014).
24. Deuretzbacher, F., Becker, D., Bjerlin, J., Reimann, S. M. & Santos, L. Quantum magnetism without lattices in strongly interacting one-dimensional spinor gases. *Phys. Rev. A* **90**, 013611 (2014).
25. Volosniev, A. G. *et al.* Engineering the dynamics of effective spin-chain models for strongly interacting atomic gases. *Phys. Rev. A* **91**, 023620 (2015).
26. Levinsen, J., Massignan, P., Bruun, G. M. & Parish, M. M. Strong-coupling ansatz for the one-dimensional Fermi gas in a harmonic potential. *Science Advances* **1** (2015).
27. Yang, L., Guan, L. & Pu, H. Strongly interacting quantum gases in one-dimensional traps. *Phys. Rev. A* **91**, 043634 (2015).
28. Hu, H., Guan, L. & Chen, S. Strongly interacting Bose-Fermi mixtures in one dimension. *New Journal of Physics* **18**, 025009 (2016).
29. Yang, L. & Cui, X. Effective spin-chain model for strongly interacting one-dimensional atomic gases with an arbitrary spin. *Phys. Rev. A* **93**, 013617 (2016).
30. Ogata, M. & Shiba, H. Bethe-ansatz wave function, momentum distribution, and spin correlation in the one-dimensional strongly correlated Hubbard model. *Phys. Rev. B* **41**, 2326–2338 (1990).
31. Busch, T., Englert, B.-G., Rzazewski, K. & Wilkens, M. Two cold atoms in a harmonic trap. *Foundations of Physics* **28**, 549–559 (1998).
32. Anderson, P. W. Infrared catastrophe in Fermi gases with local scattering potentials. *Phys. Rev. Lett.* **18**, 1049–1051 (1967).
33. Dehkharghani, A. S., Volosniev, A. G. & Zinner, N. T. Impenetrable mass-imbalanced particles in one-dimensional harmonic traps (2015). arXiv:1511.01702.
34. Loft, N. J. S., Kristensen, L. B., Thomsen, A. E. & Zinner, N. T. Comparing models for the ground state energy of a trapped one-dimensional Fermi gas with a single impurity (2015). arXiv:1508.05917.
35. Zinner, N. T., Volosniev, A. G., Fedorov, D. V., Jensen, A. S. & Valiente, M. Fractional energy states of strongly interacting bosons in one dimension. *EPL (Europhysics Letters)* **107**, 60003 (2014).
36. Massignan, P., Levinsen, J. & Parish, M. M. Magnetism in strongly interacting one-dimensional quantum mixtures. *Phys. Rev. Lett.* **115**, 247202 (2015).
37. Palzer, S., Zipkes, C., Sias, C. & Köhl, M. Quantum transport through a Tonks-Girardeau gas. *Phys. Rev. Lett.* **103**, 150601 (2009).
38. Mathy, C. J. M., Zvonarev, M. B. & Demler, E. Quantum flutter of supersonic particles in one-dimensional quantum liquids. *Nat Phys* **8**, 881–886 (2012).
39. Knap, M., Mathy, C. J. M., Ganahl, M., Zvonarev, M. B. & Demler, E. Quantum flutter: Signatures and robustness. *Phys. Rev. Lett.* **112**, 015302 (2014).
40. Farrell, A. & van Zyl, B. P. Universality of the energy spectrum for two interacting harmonically trapped ultra-cold atoms in one and two dimensions. *Journal of Physics A: Mathematical and Theoretical* **43**, 015302 (2010).
41. Harshman, N. L. Symmetries of three harmonically trapped particles in one dimension. *Phys. Rev. A* **86**, 052122 (2012).

42. Loft, N. J. S., Dehkharghani, A. S., Mehta, N. P., Volosniev, A. G. & Zinner, N. T. A variational approach to repulsively interacting three-fermion systems in a one-dimensional harmonic trap. *Eur. Phys. J D* **69**, 65 (2015).
43. Girardeau, M. D., Wright, E. M. & Triscari, J. M. Ground-state properties of a one-dimensional system of hard-core bosons in a harmonic trap. *Phys. Rev. A* **63**, 033601 (2001).
44. Gharashi, S. E., Yin, X. Y., Yan, Y. & Blume, D. One-dimensional fermi gas with a single impurity in a harmonic trap: Perturbative description of the upper branch. *Phys. Rev. A* **91**, 013620 (2015).
45. Gloeckner, D. & Lawson, R. Spurious center-of-mass motion. *Physics Letters B* **53**, 313 – 318 (1974).
46. Christensson, J., Forssén, C., Åberg, S. & Reimann, S. M. Effective-interaction approach to the many-boson problem. *Phys. Rev. A* **79**, 012707 (2009).
47. Rotureau, J. Interaction for the trapped Fermi gas from a unitary transformation of the exact two-body spectrum. *Eur. Phys. J. D* **67**, 153 (2013).
48. Lindgren, E. J., Rotureau, J., Forssén, C., Volosniev, A. G. & Zinner, N. T. Fermionization of two-component few-fermion systems in a one-dimensional harmonic trap. *New Journal of Physics* **16**, 063003 (2014).
49. Mitroy, J. *et al.* Theory and application of explicitly correlated Gaussians. *Rev. Mod. Phys.* **85**, 693–749 (2013).
50. Volosniev, A. G. *Few-Body Systems in Low-Dimensional Geometries*. Ph.D. thesis, Aarhus University, Aarhus, Denmark (2013).

Acknowledgements

Part of this work is based on the Bachelor thesis of M.E.S.A. The authors thank C. Forssén, D. V. Fedorov, and A. S. Jensen for discussions, as well as C. Forssén and X. Cui for feedback on the manuscript. We thank the experimental team of the S. Jochim group for extended discussions and for sharing their results.

This work was funded by the Danish Council for Independent Research DFF Natural Sciences and the DFF Sapere Aude program.

Author contributions statement

A.G.V., E.J.L. and N.T.Z. devised the project. M.E.S.A. and A.S.D. developed the formalism under the supervision of A.G.V. and N.T.Z. The numerical calculations were carried out by A.S.D. and M.E.S.A. with assistance from A.G.V. and E.J.L. The initial draft of the paper was written by M.E.S.A., A.S.D., and N.T.Z. All authors contributed to the revisions that led to the final version.

Additional information

The authors declare that they have no competing financial interests.

Supplementary Materials

Stationary points of trial state energy functional

For notational convenience, we define the function

$$E'(\alpha_0, \alpha_\infty) \equiv E - E_0 = \frac{\langle \gamma_0 | V | \gamma_0 \rangle \alpha_0^2 + \Delta E \alpha_\infty^2}{\alpha_0^2 + \alpha_\infty^2 + 2\langle \gamma_0 | \gamma_\infty \rangle \alpha_0 \alpha_\infty}. \quad (34)$$

Stationary points of E' are found where $(\partial E' / \partial \alpha_0, \partial E' / \partial \alpha_\infty) = (0, 0)$. This gives the system of equations

$$\begin{bmatrix} \langle \gamma_0 | V | \gamma_0 \rangle - E' & -\langle \gamma_0 | \gamma_\infty \rangle E' \\ -\langle \gamma_0 | \gamma_\infty \rangle E' & \Delta E - E' \end{bmatrix} \begin{bmatrix} \alpha_0 \\ \alpha_\infty \end{bmatrix} = 0. \quad (35)$$

For non-trivial solutions, the determinant of the above coefficient matrix must be zero. This yields the quadratic equation

$$0 = (1 - \langle \gamma_0 | \gamma_\infty \rangle^2) E'^2 - (\langle \gamma_0 | V | \gamma_0 \rangle + \Delta E) E' + \langle \gamma_0 | V | \gamma_0 \rangle \Delta E \quad (36)$$

from which we arrive at Eq. (7) of the Main Text.

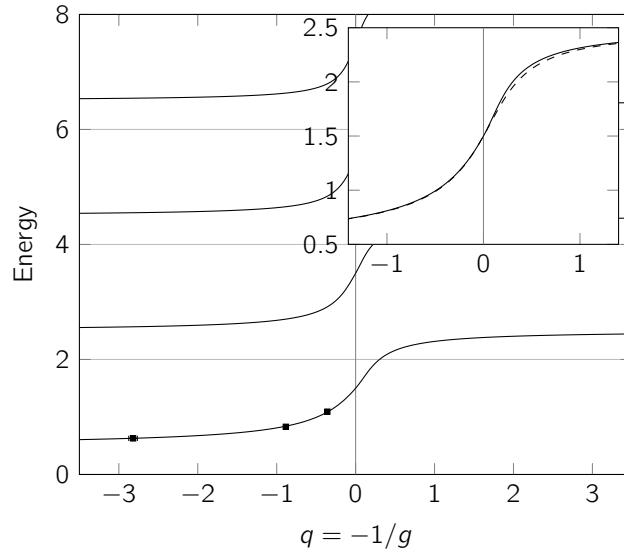


Figure 1. Energy spectrum for the two-particle system. Relative energy of two distinguishable fermions according to the interpolatory ansatz, showing the low-energy part of the spectrum. Only states with even parity are plotted as odd-parity states are not influenced by the zero-range interaction. The system also has a deeply bound state, but this is not plotted. Squares are experimental data points (note that the error bars are smaller than the data points)¹⁹. The inset is a zoom of the ground-state energy comparing the interpolatory ansatz (solid) with the exact eigenenergy (dashed) for the ground state on the repulsive side as it crosses to the attractive side.

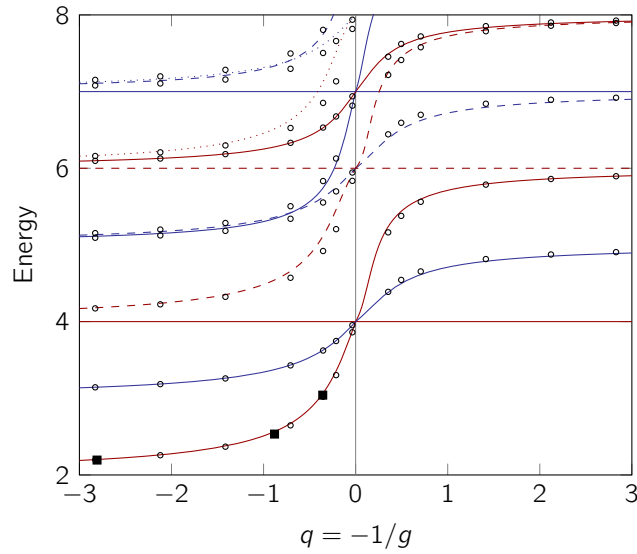


Figure 2. Energy spectrum of the interpolatory ansatz for the three-particle system. Red curves are energies of trial states with odd parity, and blue curves are those with even parity. Solid curves represent states with $\nu = 0$, dashed curves $\nu = 1$, and dotted curves $\nu = 2$. Circles are numerical calculations. Deeply bound states are excluded from the plot. Squares are experimental data-points¹⁹. The error bars on the experimental data points are smaller than the squares and are therefore not shown.

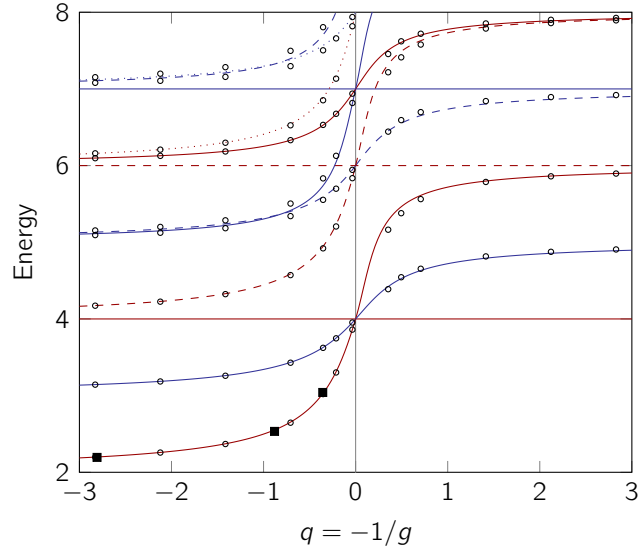


Figure 3. Energy spectrum for the three-particle system – modified ansatz. Energy spectrum for the three-particle system as in Fig. 2, but with the interpolatory ansatz modified to be perturbatively correct.

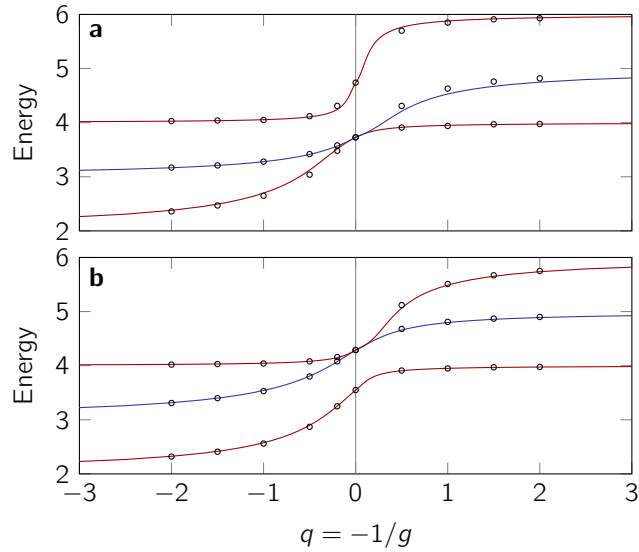


Figure 4. Energy spectrum for the three-particle system with different masses. Examples are given with mass ratio (a) $M/m = 1/2$ and (b) $M/m = 2$. Red curves indicate odd-parity states while blue curves indicate even-parity states. The circles are the exact results, calculated numerically using the correlated Gaussian method.

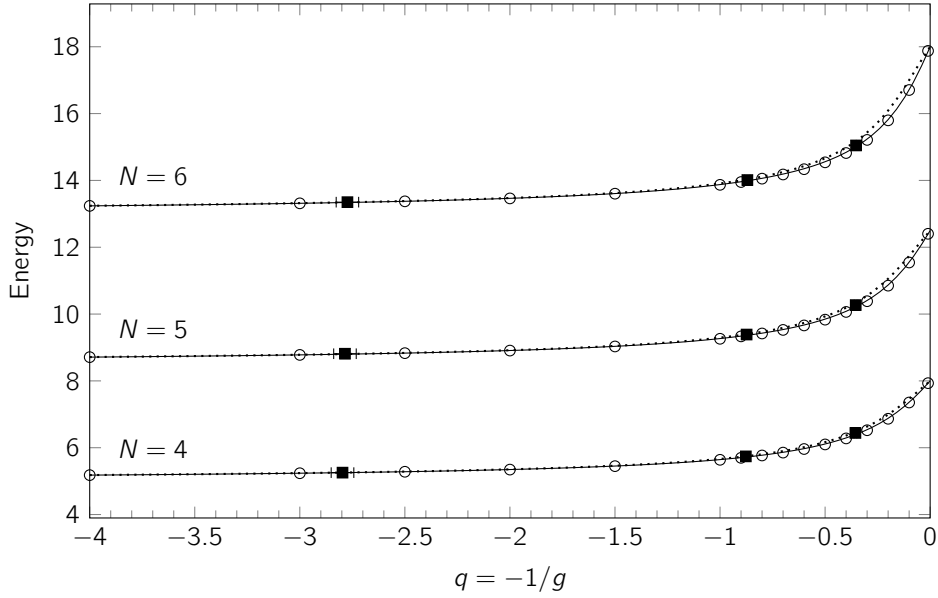


Figure 5. Energy spectrum of the impurity system. Energy of the ground state as predicted by the interpolatory ansatz with $|\gamma_\infty\rangle$ being the energy eigenstate in the $q = 0$ limit (dotted curve) and the modified ansatz (solid curve) for $N = 4, 5, 6$. This is compared with exact numerical calculations (circles) and experimental data (squares)¹⁹. Note that the error bars on the experimental data points are smaller than the squares and are only discernible for the points at small g .

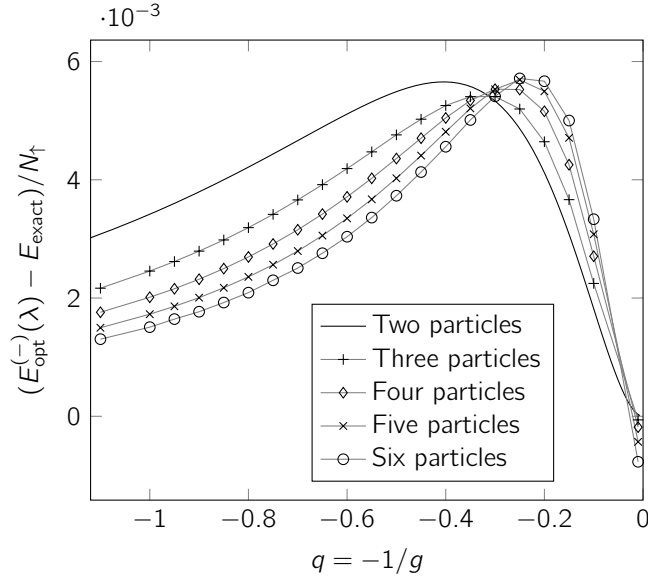


Figure 6. Ansatz accuracy comparison. Error in energy according to the modified ansatz compared to exact numerical results for impurity systems of $N = 2 - 6$ particles. (For $N = 2$ it is compared to the exact analytical solution.) For $N \geq 3$, the gray lines between the points are a mere guide to the eye. Note the scale of the vertical axis.

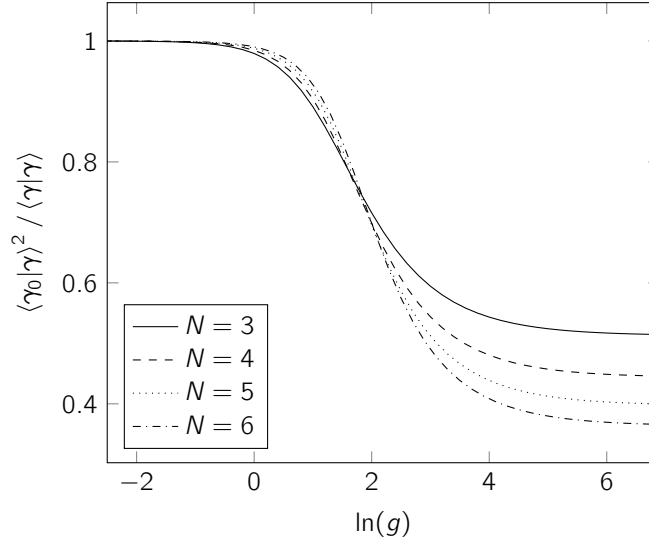


Figure 7. Anderson overlap according to the interpolatory ansatz. The (squared) overlap between the non-interacting energy eigenstate and the interacting state as a function of interaction strength for $N = 3 - 6$.

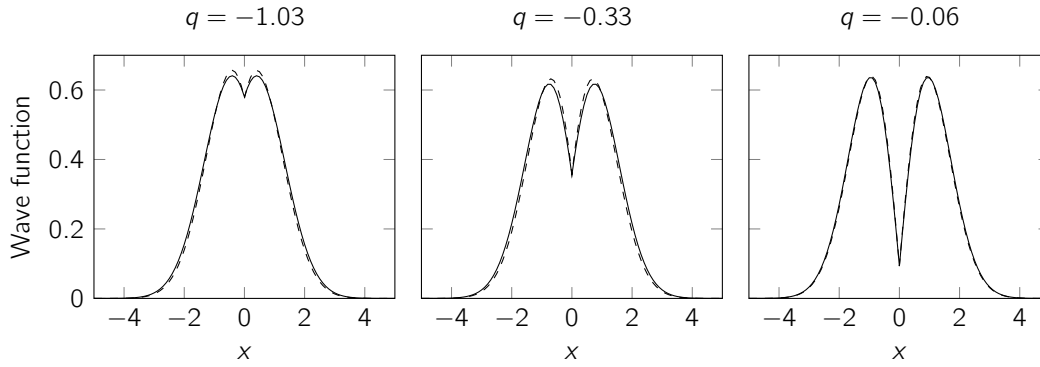


Figure 8. Wave function of the two-particle system. The ground-state wave function of the relative motion of the two particles for different values of $q = -1/g < 0$ according to the exact result (dashed) and the interpolatory ansatz (solid), respectively. The wave functions have been normalised.

If a pair, $(\alpha_0, \alpha_\infty)$, realizes a stationary point of E' , it solves Eq. (35). This condition can be reduced to the relation

$$\alpha_0 = \frac{1}{\langle \gamma_0 | \gamma_\infty \rangle} \frac{E_\infty - E}{E - E_0} \alpha_\infty. \quad (37)$$

Substituting Eq. (7) of the Main Text for E , this gives Eq. (6) of the Main Text, or equivalently, that α_0/α_∞ solves the quadratic equation

$$\langle \gamma_0 | V | \gamma_0 \rangle \langle \gamma_0 | \gamma_\infty \rangle x^2 + (\langle \gamma_0 | V | \gamma_0 \rangle - \Delta E) x - \Delta E \langle \gamma_0 | \gamma_\infty \rangle = 0. \quad (38)$$

More on the two-particle system

Wave functions

As is shown in Fig. 8, the wave function of the ground state in the $q < 0$ region as calculated with our ansatz is very similar to the exact one³¹.

Including a deeply bound state

For attractive interactions, a deeply bound molecular state exists for which the energy diverges as q approaches zero from the positive side. This state corresponds to the bound state of a delta potential well.

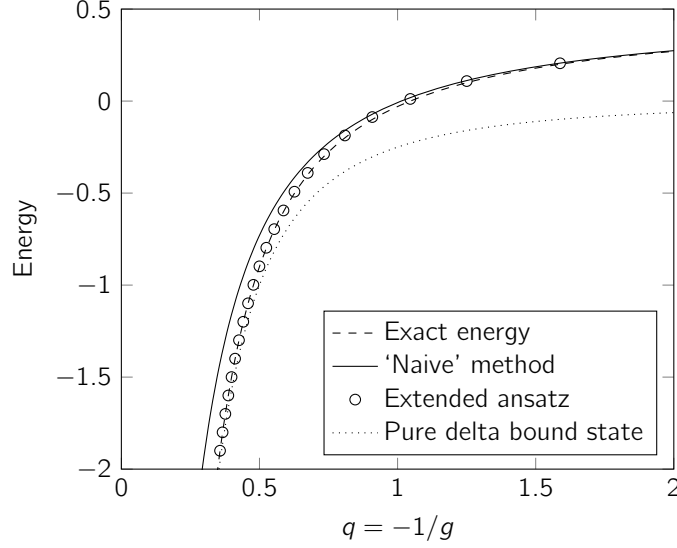


Figure 9. Energy of deeply bound state. Energy of the two-particle ground state for attractive interactions according to the exact result (dashed), the ‘naive’ interpolatory ansatz (solid) and the extended ansatz of Eq. (40) (circles), respectively. For comparison, the ground-state energy of a system without the harmonic trap is also plotted (dotted).

We may naively attempt to approximate the deeply bound state with the same trial state used for the ground state for $q < 0$; that is, Eq. (4) of the Main Text with $(n_1, n_2) = (0, 1)$. The optimised energy of this state, however, does not diverge fast enough as $g \rightarrow -\infty$. In the following, we will present a revised ansatz for the deeply bound state. Note that this is in order to improve our accuracy in the strong bound regime (large negative energy). For weaker bound states (and for repulsive interaction) the interpolatory ansatz is very accurate without additional states.

For strong attractive interactions, the wave function of the deeply bound state is densely concentrated around $x = 0$ and the length scale of the harmonic trap is very large compared to the extend of the wave function. The harmonic trap is thus neglectable when $g \ll 0$, and the wave function approaches that of a delta potential well, that is,

$$\langle x | \gamma_\delta \rangle = \sqrt{\frac{|g|}{2}} e^{-|gx|/\sqrt{2}}, \quad (39)$$

where we denote the ground state of the delta potential well by $|\gamma_\delta\rangle$ and its corresponding energy by $E = -\frac{1}{4}g^2$.

In this light, we may extend the ansatz with the additional state $|\gamma_\delta\rangle$:

$$|\gamma\rangle = \alpha_0|\gamma_0\rangle + \alpha_\infty|\gamma_\infty\rangle + \alpha_\delta|\gamma_\delta\rangle, \quad (40)$$

where $|\gamma_0\rangle = |n_1 = 0\rangle$ and $|\gamma_\infty\rangle$ is given by Eq. (21) of the Main Text with $n_2 = 1$. One might be tempted to leave out the state $|\gamma_\infty\rangle$, but this state is in fact required if the trial state is to approximate the ground state not only in the limits $g \simeq 0$ and $g \ll 0$, but also in-between.

The extended ansatz gives rise to a cubic equation containing error functions, and we have solved this numerically. The resulting energy is shown in Fig. 9 and is in much better agreement with the exact energy than the original ansatz. The wave function of the extended ansatz is also very close to the exact wave function. This is evident from Fig. 10, comparing the two wave functions for three values of q .

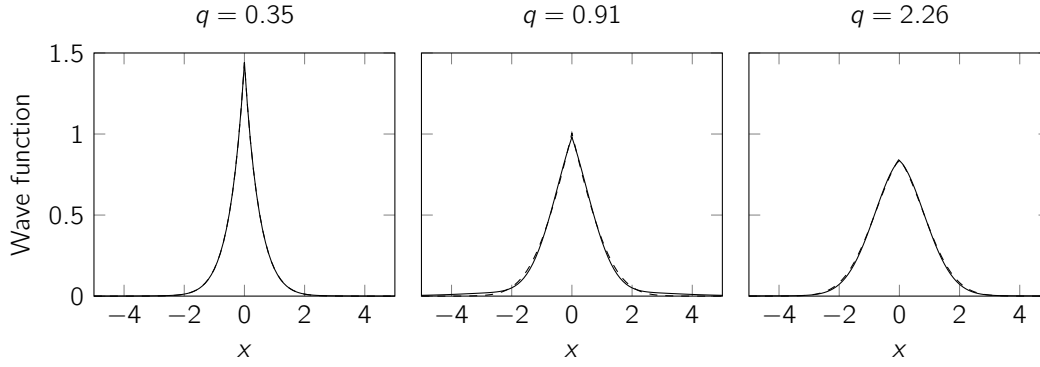


Figure 10. Wave function of deeply bound state. The two-particle ground-state wave function for different values of $q = -1/g > 0$ according to the exact result (dashed) and the extended ansatz of Eq. (40) (solid), respectively. The wave functions have been normalised.

Details of the impurity system

Denote the wave function of the n 'th excited state of the single-particle harmonic oscillator ψ_n and define the Slater determinant⁴³

$$F(\psi_0, \dots, \psi_{N-1}; x_1, \dots, x_N) \equiv \frac{1}{\sqrt{N!}} \det \begin{bmatrix} \psi_0(x_1) & \psi_0(x_2) & \dots & \psi_0(x_N) \\ \psi_1(x_1) & \psi_1(x_2) & \dots & \psi_1(x_N) \\ \vdots & \vdots & \ddots & \vdots \\ \psi_{N-1}(x_1) & \psi_{N-1}(x_2) & \dots & \psi_{N-1}(x_N) \end{bmatrix} \quad (41)$$

$$= \left(\frac{2^{N-1}}{\pi} \right)^{N/4} \frac{1}{\sqrt{N!}} \left(\prod_{n=0}^{N-1} \frac{1}{\sqrt{n!}} \right) e^{-\mathbf{x}^2/2} \prod_{1 \leq j < k \leq N} (x_k - x_j). \quad (42)$$

The ground state in the non-interacting limit has energy $E_0 = (N_{\uparrow}^2 + 1)/2$, and with the notation defined above,

$$\langle \mathbf{x} | \gamma_0 \rangle = \psi_0(x_1) F(\psi_0, \dots, \psi_{N-2}; x_2, \dots, x_N). \quad (43)$$

Meanwhile, the completely antisymmetric state has wave function

$$\langle \mathbf{x} | \gamma_A \rangle = F(\psi_0, \dots, \psi_{N-1}; x_1, \dots, x_N) \quad (44)$$

and energy $E_{\infty} = N^2/2$.

The interaction energy in the non-interacting state is

$$\langle \gamma_0 | V | \gamma_0 \rangle = (N-1)g \int_{-\infty}^{\infty} dx_1 \int_{-\infty}^{\infty} dx_2 \int_{-\infty}^{\infty} dx_3 \dots \int_{-\infty}^{\infty} dx_N \langle \mathbf{x} | \gamma_0 \rangle^2 |_{x_2=x_1}. \quad (45)$$

For the ground state, this reduces to⁴⁴

$$\langle \gamma_0 | V | \gamma_0 \rangle = \frac{\sqrt{2}}{\pi(N-2)!} \Gamma(N-1/2)g. \quad (46)$$

Using Eq. (16) of the Main Text, the $\langle \gamma_0 | \gamma_{\infty} \rangle$ may be calculated through

$$\langle \gamma_0 | \gamma_A \rangle_n = \binom{N-1}{n-1} \int_{-\infty}^{\infty} dx_1 \int_{-\infty}^{x_1} dx_2 \dots \int_{-\infty}^{x_1} dx_n \int_{x_1}^{\infty} dx_{n+1} \dots \int_{x_1}^{\infty} dx_N \langle \gamma_0 | \mathbf{x} \rangle \langle \mathbf{x} | \gamma_A \rangle. \quad (47)$$

Slope of energy curve

The slope of the ground-state energy curve at $g \rightarrow \infty$ is the greatest eigenvalue of the matrix²²

$$\mathbf{A} = \begin{bmatrix} \alpha_1 & -\alpha_1 & 0 & 0 & \dots & 0 & 0 & 0 \\ -\alpha_1 & \alpha_1 + \alpha_2 & -\alpha_2 & 0 & \dots & 0 & 0 & 0 \\ 0 & -\alpha_2 & \alpha_2 + \alpha_3 & -\alpha_3 & \dots & 0 & 0 & 0 \\ \vdots & \vdots & \vdots & \vdots & \ddots & \vdots & \vdots & \vdots \\ 0 & 0 & 0 & 0 & \dots & -\alpha_2 & \alpha_1 + \alpha_2 & -\alpha_1 \\ 0 & 0 & 0 & 0 & \dots & 0 & -\alpha_1 & \alpha_1 \end{bmatrix} \quad (48)$$

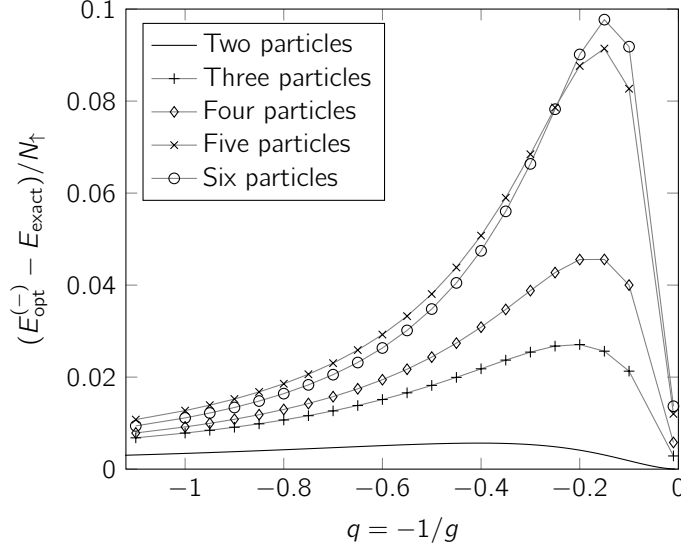


Figure 11. Accuracy of the interpolatory ansatz applied to an impurity system. Error in energy according to the unmodified interpolatory ansatz compared to exact numerical results for impurity systems of $N = 2 - 6$ particles. (For $N = 2$ it is compared to the exact analytical solution.) For $N \geq 3$, the gray lines between the points are a mere guide to the eye.

where

$$\alpha_n = \frac{N!}{(n-1)!(N-1-n)!} \int_{-\infty}^{\infty} dx_1 \int_{-\infty}^{x_1} dx_3 \cdots \int_{-\infty}^{x_1} dx_{n+1} \int_{x_1}^{\infty} dx_{n+2} \cdots \int_{x_1}^{\infty} dx_N \left(\frac{\langle \mathbf{x} | \gamma_A \rangle}{x_1 - x_2} \Big|_{x_2=x_1} \right)^2. \quad (49)$$

The coefficients, a_n , in Eq. (16) of the Main Text are the components of the eigenvector of \mathbf{A} corresponding to the greatest eigenvalue. Note that $\alpha_n = \alpha_{N+1-n}$, which is the origin of the bisymmetry of \mathbf{A} .

Error in energy of interpolatory ansatz

Figure 11 shows the error in the energy of the unmodified interpolatory ansatz compared to exact numerical methods.

Optimum wave-function overlap

By Eq. (16) of the Main Text, the squared overlap is given by

$$\langle \gamma_0 | \gamma_{\infty}(\mathbf{a}) \rangle^2 = \frac{N}{\sum_{k=1}^N a_k^2} \left(\sum_{n=1}^N a_n \langle \gamma_0 | \gamma_A \rangle_n \right)^2. \quad (50)$$

Differentiating this with respect to a coefficient, a_m , and setting the result equal to zero, we get

$$0 = N \langle \gamma_0 | \gamma_A \rangle_m \sum_{n=1}^N a_n \langle \gamma_0 | \gamma_A \rangle_n - a_m \langle \gamma_0 | \gamma_{\infty}(\mathbf{a}_{\max}) \rangle^2, \quad (51)$$

which is valid for $m = 1, \dots, N$. Thus, we arrive at the matrix equation

$$\left(N \left[\langle \gamma_0 | \gamma_A \rangle_i \langle \gamma_0 | \gamma_A \rangle_j \right]_{ij} - \langle \gamma_0 | \gamma_{\infty}(\mathbf{a}_{\max}) \rangle^2 \right) \mathbf{a} = 0. \quad (52)$$

This means that $\langle \gamma_0 | \gamma_{\infty}(\mathbf{a}_{\max}) \rangle^2$ and \mathbf{a}_{\max} is an eigenvalue and a corresponding eigenvector of the matrix

$$N \left[\langle \gamma_0 | \gamma_A \rangle_i \langle \gamma_0 | \gamma_A \rangle_j \right]_{ij} = N \begin{bmatrix} \langle \gamma_0 | \gamma_A \rangle_1 \\ \langle \gamma_0 | \gamma_A \rangle_2 \\ \vdots \\ \langle \gamma_0 | \gamma_A \rangle_N \end{bmatrix} \begin{bmatrix} \langle \gamma_0 | \gamma_A \rangle_1 & \langle \gamma_0 | \gamma_A \rangle_2 & \cdots & \langle \gamma_0 | \gamma_A \rangle_N \end{bmatrix}. \quad (53)$$

It is clear that the only non-zero eigenvalue belongs to the eigenvector $\mathbf{a}_{\max} = (\langle \gamma_0 | \gamma_A \rangle_1, \dots, \langle \gamma_0 | \gamma_A \rangle_N)$ and is as given in Eq. (17) of the Main Text; for there exist $N - 1$ vectors orthogonal to \mathbf{a}_{\max} , each being an eigenvector with eigenvalue 0.

Numerical methods

Effective interaction approach

We consider a two-component system with N_A particles in one component and N_B particles in another, the so-called $N_A + N_B$ system. Intra-species interactions are neglected, and all the particles are assumed to have the same mass, m , and trapping frequency, ω . The general Hamiltonian of the system can then be written as:

$$\mathcal{H} = \sum_{i=1}^{N_A} \left(\frac{p_{A,i}^2}{2m} + \frac{m\omega^2}{2} q_{A,i}^2 \right) + \sum_{i=1}^{N_B} \left(\frac{p_{B,i}^2}{2m} + \frac{m\omega^2}{2} q_{B,i}^2 \right) + \sum_{i_A=0}^{N_A} \sum_{i_B=0}^{N_B} V_{i_A, i_B} \quad (54)$$

where $V_{i_A, i_B} = g\delta(q_{i_A} - q_{i_B})$ are the interaction terms (g being the interaction strength), and the first two parentheses are the non-interacting part of the Hamiltonian; call it H_0 . $p_{k,i}$ and $q_{k,i}$ are the momentum and coordinate operators, respectively, for particle i in subsystem $k \in \{A, B\}$. They each operate in their own subspace, so $p_{A,i} = p_i \otimes 1$ and $p_{B,i} = 1 \otimes p_i$.

The total many-body basis state is a tensor product of many-body states from each species. We refer to the states from each subsystem as few-body states and to states describing the full system as many-body states. In each subsystem we have identical fermions and therefore we need a totally antisymmetric few-body state, that is, a state that is antisymmetric under the exchange of *any two* particles:

$$|(m_1 m_2 \dots m_N)\rangle \equiv \frac{1}{\sqrt{N!}} \sum_{\sigma \in S_N} |m_{\sigma(1)}\rangle |m_{\sigma(2)}\rangle \dots |m_{\sigma(N)}\rangle, \quad (55)$$

where we choose $m_1 > m_2 > \dots > m_N$ by convention and S_N is the symmetric group of order N . The $|m_i\rangle$ represents a single-particle state equivalent to a harmonic oscillator eigenstate corresponding to eigenvalue m_i with respect to the number operator $a_i^\dagger a_i$. These single-particle states are convenient to use since they are eigenstates of H_0 . The complete basis for the full system can thus be written as

$$|\Psi\rangle = |(m_1 m_2 \dots m_{N_A})\rangle \otimes |(k_1 k_2 \dots k_{N_B})\rangle. \quad (56)$$

The corresponding eigenvalue to H_0 is $E = \hbar\omega(\frac{N_A + N_B}{2} + m_1 + \dots + m_{N_A} + k_1 + \dots + k_{N_B})$.

One of the nice properties of the Hamiltonian is that its kinetic energy and harmonic trap operators are one-particle operators, and only the interaction operator couples the particles. This means that the overall matrix is actually a sparse matrix. By construction, the contribution of the kinetic energy and harmonic trap terms are trivial. However, the interaction part is given as

$$M = \text{sgn}[\sigma\tau\sigma'\tau'] V_{n_{\sigma(1)}, h_{\tau(1)}, n'_{\sigma'(1)}, h'_{\tau'(1)}}, \quad (57)$$

where $V_{a,b,c,d} \equiv \langle a, b | V | c, d \rangle$ is the two-body subspace matrix element and sgn is the sign function, which comes from how many times the states are swapped with each other. In addition, we are only interested in the intrinsic dynamics of states, therefore we use a Lawson projection term⁴⁵ to push away the many-body solutions corresponding to excitations of the center of mass.

An effective two-body interaction is considered instead of the bare zero-range interaction. The advantage of this effective interaction is that it converges rapidly as a function of model space size. This has been utilized to address cold atomic gases in recent papers^{46,47}. It is constructed in a truncated two-body space, P , defined as the set of two-body relative harmonic oscillator states whose radial quantum numbers are smaller than a cutoff, n_{\max} , and it is designed such that its solutions correspond to the two-body energies that are given by the Busch formula³¹. The unitary transformation of the constructed two-body effective Hamiltonian is given as⁴⁸

$$H_p^{\text{eff}} = \frac{U_{PP}^\dagger}{\sqrt{(U_{PP}^\dagger U_{PP})}} E_{PP}^{(2)} \frac{U_{PP}}{\sqrt{(U_{PP}^\dagger U_{PP})}} \quad (58)$$

where $E_{PP}^{(2)}$ is the diagonal matrix with eigenvalues from the P -space and U_{PP} is the matrix whose rows are formed by the corresponding eigenvectors. In the limit of infinite model space, $n_{\max} \rightarrow \infty$, the unitary transformation approaches the exact bare Hamiltonian results. However, the convergence to the exact limit is a lot quicker than expected for small systems. For example, $n_{\max} = 20$ for the $2 + 1$ system is more than enough to obtain results with a precision of 3 decimals and only a few minutes of calculation time.

Correlated Gaussian approach

Here we present the details of the correlated Gaussian approach that we have employed for the mass-imbalanced case. For further details on this method see Ref.⁴⁹. We consider a general Hamiltonian given as

$$\mathcal{H} = \sum_{i=1}^{N_{\text{tot}}} \left(\frac{p_i^2}{2m_i} + V_{\text{ext}}(x_i) \right) + \sum_{i<j} V(x_i, x_j), \quad (59)$$

where x_i is the coordinate of the i 'th particle, $V_{\text{ext}}(x_i)$ is the external confinement and $V(x_i, x_j)$ is the 2-body interaction potential. In our case $V_{\text{ext}}(x_i) = \frac{1}{2}m\omega^2 x_i^2$ and $V(x_i, x_j) = g\delta(x_i - x_j)$, with g being the interaction strength. Please note that the specified potentials are not crucial for the method and any other system with vanishing 2-body potential for larger separation and any bounded external potential could easily do. An upper limit for the bound ground state can be found variationally based on the functional

$$E_{\text{upper}}[f] = \frac{\langle f | H | f \rangle}{\langle f | f \rangle}, \quad (60)$$

where $|f\rangle$ is a normalizable and differentiable function built as a linear combination of states from a basis $\{\phi_k\}$: $|f\rangle = \sum_{k=1}^l c_k \phi_k$, where l is a computationally accessible number that is set to reach a given precision. We use a basis in the form of Gaussian functions,

$$\phi_k = e^{-(x_j - s_j^k) A_{jf}^k (x_f - s_f^k)} \equiv e^{-(\mathbf{x} - \mathbf{s})^T \mathbf{A} (\mathbf{x} - \mathbf{s}')}, \quad (61)$$

where $\{x_j\}$ are the coordinates of the system while s_j^k and A_{jf}^k are numbers that characterize the basis elements. In order to ensure square-integrability we assume A_{jf}^k is symmetric and positive-definite. Note that Einstein's repeated summation notation is used here.

Gaussian functions usually have an analytical expression when one wants to calculate for instance $\langle \phi_k | \phi_k \rangle$ or $\langle \phi_k | \frac{\partial^2}{\partial x^2} | \phi_k \rangle$, making it very fast to calculate such expressions numerically. These functions can also be transformed easily from one Jacobi coordinate set to another and even any desirable features such as symmetry can be implemented into the ansatz.

Our next step is to choose a subset of l elements from a complete basis. This can be done in many ways, deterministically, randomly or a mix. In our calculations, we choose the first k elements with $k < l$ stochastically. This subset is the starting point of the trial function. We generate A_{jl}^k and s_j^k randomly from an appropriate distribution (e.g. exponential or Laplacian) and then determine the upper bound for the ground state. We can choose to do this step several times, say α times, and then among these α times we choose the best trial function with the lowest trial energy, call it k_{best} . Then we can start to expand k_{best} by adding some other elements randomly created, $k_{\text{best}} \mapsto k_{\text{best}} + k_{\text{add}} \leq l$ and by doing so, say β times, and then again picking the lowest energy among the β trials as our new candidate, we end up constructing a trial function that has an upper bound for the ground-state energy.

One should note, that in some situations where the functions do not decay fast enough at infinity or there are some delta functions, the number of elements in the finite basis has to be very large or go to infinity in order to describe the exact wave function everywhere. For the convergence and error of this method, see Ref.⁵⁰. However, the method used here for our system converges relatively fast with a precision up to 4 decimals with the parameters $\alpha = 500$ and $\beta = 500$ and a calculation time of approximately 1 hour.

In order to illustrate the method, we look at our Hamiltonian for the mass-imbalanced 2 + 1 system given in relative coordinates:

$$H_{\text{rel}} = T_{\text{rel}} + V_{\text{ext,rel}} + \sum_{i<j} V_{ij} \quad (62)$$

where $T_{\text{rel}} = \frac{1}{2}(p_{x_1'}^2 + p_{x_2'}^2)$, $V_{\text{ext,rel}} = \frac{1}{2}(x_1'^2 + x_2'^2)$ and

$$\sum_{i<j} V_{ij} = \frac{g}{\hbar\omega\sigma} \left[\frac{\mu_{23}}{\sqrt{\mu}} \delta(x_1') + \frac{\sqrt{\mu}}{\mu_{23}} \delta\left(\frac{\mu}{m_1} x_1' + x_2'\right) + \frac{\sqrt{\mu}}{\mu_{23}} \delta\left(-\frac{\mu}{m_2} x_1' + x_2'\right) \right], \quad (63)$$

with x_1' , x_2' , σ , μ and μ_{23} defined as in the treatment of the mass-imbalanced system in the main text. We ignore the center-of-mass Hamiltonian because its solutions are already known.

With this Hamiltonian, we can calculate the following quantities:

$$N_{ij} \equiv \langle \phi_i | \phi_j \rangle = \exp\left(-(\mathbf{s}^T \mathbf{A} \mathbf{s} + \mathbf{s}'^T \mathbf{A}' \mathbf{s}') + \frac{1}{4} \mathbf{v}^T (\mathbf{B}^{-1})^T \mathbf{v}\right) \frac{\pi^{3/2}}{\sqrt{\det(\mathbf{B})}} \quad (64)$$

$$T_{\text{rel}} = \frac{1}{2} \langle \phi_i | \mathbf{p}^T \mathbf{p} | \phi_j \rangle = \frac{1}{2} N_{ij} (\text{Tr}(\mathbf{A}') - \text{Tr}(\mathbf{A}'^2 \mathbf{B}^{-1}) - 2\alpha^T \mathbf{A}'^2 \alpha + 4\mathbf{s}'^T \mathbf{A}'^2 \alpha - 2\mathbf{s}'^T \mathbf{A}'^2 \mathbf{s}') \quad (65)$$

$$V_{\text{ext,rel}} = \frac{1}{2} \langle \phi_i | \mathbf{x}_1'^T \mathbf{x} | \phi_j \rangle = \frac{1}{2} N_{ij} \left(\frac{1}{2} \text{Tr}(\mathbf{B}^{-1}) + \frac{1}{4} \mathbf{v}^T (\mathbf{B}^{-1})^2 \mathbf{v} \right) \quad (66)$$

$$\langle \phi_i | \delta(x) | \phi_j \rangle = \frac{\sqrt{\det(\mathbf{B})}}{\pi^{3/2}} N_{ij} \exp \left(-\det(\mathbf{B}) \frac{\alpha_1^2}{B_{22}} \right) \quad (67)$$

$$\langle \phi_i | \delta \left(\pm \frac{\mu}{m} x'_1 + x'_2 \right) | \phi_j \rangle = \frac{\sqrt{\det(\mathbf{B})}}{\pi^{3/2}} N_{ij} \frac{m}{\mu} \frac{\sqrt{\pi}}{\sqrt{B_{22} + \frac{m^2}{\mu^2} B_{11} \mp \frac{m}{\mu} 2B_{12}}} \exp \left(-\det(\mathbf{B}) \frac{(\alpha_1 \pm \frac{m}{\mu} \alpha_2)^2}{B_{22} + \frac{m^2}{\mu^2} B_{11} \mp \frac{m}{\mu} 2B_{12}} \right), \quad (68)$$

where $\mathbf{B} = \mathbf{A} + \mathbf{A}'$, $\mathbf{v} = 2(\mathbf{A}\mathbf{s} + \mathbf{A}'\mathbf{s}')$, $\alpha = \frac{1}{2}\mathbf{B}^{-1}\mathbf{v}$ and $m_2 = m_3 = m$. The analytical expressions for each of the integrals make it easy to calculate the value of $\langle f | H | f \rangle$ fast numerically and then try this several times for some randomly generated ansatz. In this way we can find a close upper limit to the ground-state energy of our Hamiltonian.